blood®
Regular Article

LYMPHOID NEOPLASIA

Development and survival of MYC-driven lymphomas require the MYC antagonist MNT to curb MYC-induced apoptosis

Hai Vu Nguyen,[1,2,*] Cassandra J. Vandenberg,[1,2,*] Ashley P. Ng,[1,2] Mikara R. Robati,[1] Natasha S. Anstee,[1,2] Joel Rimes,[1,2] Edwin D. Hawkins,[1,2] and Suzanne Cory[1,2]

[1]The Walter and Eliza Hall Institute of Medical Research, Melbourne, VIC, Australia; and [2]Department of Medical Biology, University of Melbourne, Melbourne, VIC, Australia

KEY POINTS

- MNT aids MYC-driven B lymphomagenesis by curbing MYC-induced apoptosis, primarily through suppressing BIM.
- Induced MNT loss in transplanted Eμ-*Myc* lymphomas extends recipient survival, making MNT a novel therapeutic target for MYC-driven tumors.

Deregulated overexpression of MYC is implicated in the development and malignant progression of most (~70%) human tumors. MYC drives cell growth and proliferation, but also, at high levels, promotes apoptosis. Here, we report that the proliferative capacity of MYC-driven normal and neoplastic B lymphoid cells depends on MNT, a MYC-related transcriptional repressor. Our genetic data establish that MNT synergizes with MYC by suppressing MYC-driven apoptosis, and that it does so primarily by reducing the level of pro-apoptotic BIM. In Eμ-*Myc* mice, which model the *MYC/IGH* chromosome translocation in Burkitt's lymphoma, homozygous *Mnt* deletion greatly reduced lymphoma incidence by enhancing apoptosis and markedly decreasing premalignant B lymphoid cell populations. Strikingly, by inducing *Mnt* deletion within transplanted fully malignant Eμ-*Myc* lymphoma cells, we significantly extended transplant recipient survival. The dependency of lymphomas on MNT for survival suggests that drugs inhibiting MNT could significantly boost therapy of MYC-driven tumors by enhancing intrinsic MYC-driven apoptosis. (*Blood*. 2020;135(13):1019-1031)

Introduction

The transcription factor c-MYC (hereafter MYC) regulates expression of a multitude of genes involved in cell growth, proliferation, metabolism, and the DNA damage response.[1] In normal cells, the level of MYC is tightly regulated, but in cancer cells, it is almost always elevated and constitutive.[2,3] Although not fully transforming, MYC overexpression provides a strong drive toward malignancy.[4] Importantly, however, MYC's oncogenic potential is tempered by its propensity to induce apoptosis in cells stressed by inadequate access to cytokines or nutrients,[5,6] particularly at high MYC levels.[7] Mutations that inhibit apoptosis therefore synergize with MYC in tumorigenesis, as first shown for anti-apoptotic BCL-2.[8,9]

MYC and its closest relatives, N-MYC and L-MYC, bind DNA at canonical CACGTG E-boxes (and noncanonical variants) as a heterodimer with MAX, a related basic helix-loop-helix leucine zipper (bHLHLZ) protein.[1] MYC:MAX heterodimers can activate[10] or repress[11] hundreds of genes,[12] although many may be indirect targets.[13] MYC action is opposed by other bHLHLZ relatives such as the 4 MXD proteins and MNT, which also heterodimerize with MAX and bind to E-boxes in many promoters and enhancers. By interacting with SIN3 proteins, MXD/MNT proteins recruit histone deacetylase-containing complexes to repress target genes.[1]

MNT[14,15] is evolutionarily conserved and widely expressed during development and in adult tissues. Certain genes targeted by MYC:MAX heterodimers are also targets of MNT:MAX heterodimers.[16] Genetic loss or knockdown of MNT was reported to enhance proliferation, increase RAS-induced transformation, and augment sensitivity to apoptotic stimuli, all characteristics of MYC overexpression.[17-19] Therefore, MNT was posited as a tumor suppressor, a role supported by early mouse studies showing that its tissue-specific loss produced mammary adenocarcinomas[20] and thymic lymphomas.[21] Furthermore, MNT deletions have been noted in a variety of human cancers,[22] including chronic lymphocytic leukemia[23] and Sezary syndrome, a cutaneous T-cell lymphoma/leukemia.[24]

Surprisingly, however, recent studies indicate that MNT actually facilitates MYC-driven tumorigenesis, rather than acting as a tumor suppressor. Thus, Hurlin's group found that T-cell-specific homozygous *Mnt* deletion prevented thymic lymphoma development in mice expressing a hypermorphic MYC protein (MYC^{T58A}) in T cells,[25] and we found that *Mnt* heterozygosity slowed T lymphomagenesis in VavP-*Myc*10^{hom} mice and B lymphomagenesis in Eμ-*Myc* mice,[26] which model the c-*MYC/IGH* chromosome translocations that hallmark Burkitt's lymphomas.[4] Link et al showed that MNT-null thymocytes expressing MYC^{T58A}

were more susceptible to apoptosis and proposed that MNT's dominant physiological role is to suppress MYC-driven apoptosis.[25] However, pre-B cells from *Mnt*$^{+/-}$ Eμ-*Myc* mice were not discernibly more sensitive to apoptosis than those from *Mnt*$^{+/+}$ Eμ-*Myc* mice.[26]

To clarify the roles of MNT in B lymphopoiesis and lymphomagenesis, we have now undertaken conditional homozygous deletion of floxed *Mnt* alleles in wild-type (WT) and Eμ-*Myc* transgenic mice. In Eμ-*Myc* mice,[4,27,28] constitutive *Myc* overexpression in B lymphoid cells, driven by the immunoglobulin H (IgH) enhancer Eμ, produces a polyclonal expansion of cycling nonmalignant pre-B cells, and every mouse goes on to develop a monoclonal malignant (transplantable) pre-B or B lymphoma harboring cooperating oncogenic mutations.[29-31]

We report here that B lymphopoiesis in both normal and Eμ-*Myc* mice is strikingly dependent on MNT. In its absence, B lymphoid cells are highly susceptible to apoptosis, largely as a result of upregulation of the BH3-only protein BIM, a potent proapoptotic BCL-2 family member.[32,33] We show that *Mnt* deletion in Eμ-*Myc* mice greatly impedes B lymphomagenesis, and that inducing *Mnt* deletion in transplanted fully malignant Eμ-*Myc* lymphoma cells extends the survival of transplant recipients. These data provide genetic proof of principle that MNT would be an effective target for therapy of MYC-driven tumors.

Materials and methods

Mice

Mice used were Eμ-*Myc*,[4,28] *Bim*$^{-/-}$del339/1,[34] *Rag1Cre*,[35] *Rosa26.CreERT2*,[36] and *Mnt*$^{fl/+}$,[37] all on a C57BL/6 background. To activate CreER recombinase in *Rosa26.CreERT2* mice, 5-week-old animals were given 200 mg/kg tamoxifen (T5648, Sigma-Aldrich) daily for 3 days by oral gavage, and analyzed after 4 weeks.

Nondecalcified long bone immunofluorescence

Immunofluorescence analysis was performed on long bone prepared without decalcification to maintain collagen signal, as described previously[38,39] and in supplemental Methods, available on the *Blood* Web site. Quantification using ImageJ/FIJI "Analyze particle" function was performed blinded to genotype.

Statistical analysis

Statistical comparisons were made using unpaired 2-tailed Student's *t*-test or analysis of variance with Prism v8.0 software (GraphPad, San Diego, CA), with P values $\leq .05$ considered statistically significant. Mouse survival analysis was carried out using GraphPad Prism (Version 8.0), and significance determined using log-rank (Mantel-Cox) test.

Results

Mnt deletion largely prevents lymphomagenesis in Eμ-*Myc* mice

To investigate the physiological role of MNT in B lymphomagenesis and avoid the early embryonic lethality of homozygous *Mnt* deletion (~E10 in C57BL/6 mice; K. J. Campbell, C.J.V., and S.C., unpublished results), we bred Eμ-*Myc*[4] mice bearing floxed *Mnt* alleles (*Mnt*$^{fl/fl}$)[37] and the *Rag1Cre*[35] transgene, which expresses Cre recombinase only in lymphoid progenitor cells.

Lymphoid-specific *Mnt* deletion strikingly reduced lymphomagenesis in Eμ-*Myc* mice (Figure 1A). *Mnt*$^{fl/fl}$ Eμ-*Myc/Rag1Cre* mice (blue curve) had a median survival of more than 400 days vs only 86 and 96 days, respectively, for Eμ-*Myc* (red) and Eμ-*Myc/Rag1Cre* (purple) mice. Consistent with our earlier study of *Mnt*$^{+/-}$ Eμ-*Myc* mice,[26] mouse survival was also significantly extended in Eμ-*Myc* mice heterozygous for *Mnt* deletion (*Mnt*$^{fl/+}$ Eμ-*Myc/Rag1Cre* mice, lime green curve; median survival, 138 days).

Most tumors that did arise in *Mnt*$^{fl/fl}$ Eμ-*Myc/Rag1Cre* mice were pre-B or B lymphomas, which is typical for Eμ-*Myc* mice, although a few seemed more differentiated (supplemental Table 1). The tumor burden was comparable in sick *Mnt*$^{fl/fl}$ Eμ-*Myc/Rag1Cre* mice and *Mnt*$^{+/+}$ Eμ-*Myc/Rag1Cre* mice (supplemental Figure 1A-B) although the *Mnt*-deleted tumors were less frequently accompanied by leukemia (2/13 [15%] versus 25/34 [74%]; supplemental Figure 1B, panel 1). Most tumors analyzed (10/13, 77%) lacked detectable MNT at either the DNA or protein level, with the other 3 having escaped *Mnt* deletion by loss (#344) or aberrant activity (#611, #340) of the *Rag1Cre* transgene (supplemental Figure 1C; supplemental Table 1). Inactivation of the p19Arf/p53 pathway in MNT-null tumors (4/10, 40%) was similar to that reported for conventional Eμ-*Myc* lymphomas (supplemental Figure 1C),[30,40] suggesting that selection against p53 is no higher in MNT-deficient than in MNT-proficient lymphomas.

Overall, these data indicate that MNT expression is highly advantageous for MYC-driven B lymphomagenesis.

Mnt deletion mediated by *Rag1Cre* provokes severe B lymphopenia in young Eμ-*Myc* mice

To investigate why MNT loss profoundly reduced lymphomagenesis in Eμ-*Myc* mice, we analyzed their premalignant phase. First, we compared expression of MNT and MYC protein in B lymphoid progenitor populations sorted from the bone marrow of young (4-week-old) WT and Eμ-*Myc* mice (supplemental Figure 2A). Transgenic MYC protein was low in pre-pro-B cells, but high in pro-B, pre-B, and recirculating IgM$^+$ B cells, whereas endogenous MYC was below the detection limit. MNT was readily detectable in pre-pro-B cells from both WT and Eμ-*Myc* mice, and its level increased substantially with maturation. Quantification of intracellular MNT by flow cytometry indicated that MNT was 2.5- to 3-fold higher in Eμ-*Myc* pro-B, pre-B, and IgM$^+$ cells than in their WT counterparts (supplemental Figure 2B).

Rag1Cre-mediated deletion of floxed *Mnt* was highly efficient, as shown by polymerase chain reaction (PCR) analysis of pro-B and pre-B cells (Figure 1B). The loss of MNT induced severe B lymphopenia in young Eμ-*Myc* mice. The several-fold increase in immature B lymphoid (B220$^+$IgM$^-$) cells normally seen in the bone marrow of young Eμ-*Myc* mice (red, purple bars)[27] was nullified by the *Mnt* deletion in *Mnt*$^{fl/fl}$ Eμ-*Myc/Rag1*Cre mice (blue bar; Figure 1C, panel 1; supplemental Figure 3A). Although pro-B and pre-B cells were both reduced ~5-fold, the more immature pre-pro-B cell progenitors (in which *Rag1*-driven *Cre* expression is marginal) were unaffected (Figure 1C, panels 2-4). The MNT-null phenotype was even more extreme in the spleen (Figure 1D), where B lymphoid cells (B220$^+$) were barely detectable, and the deficit affected all major subpopulations: pre-B

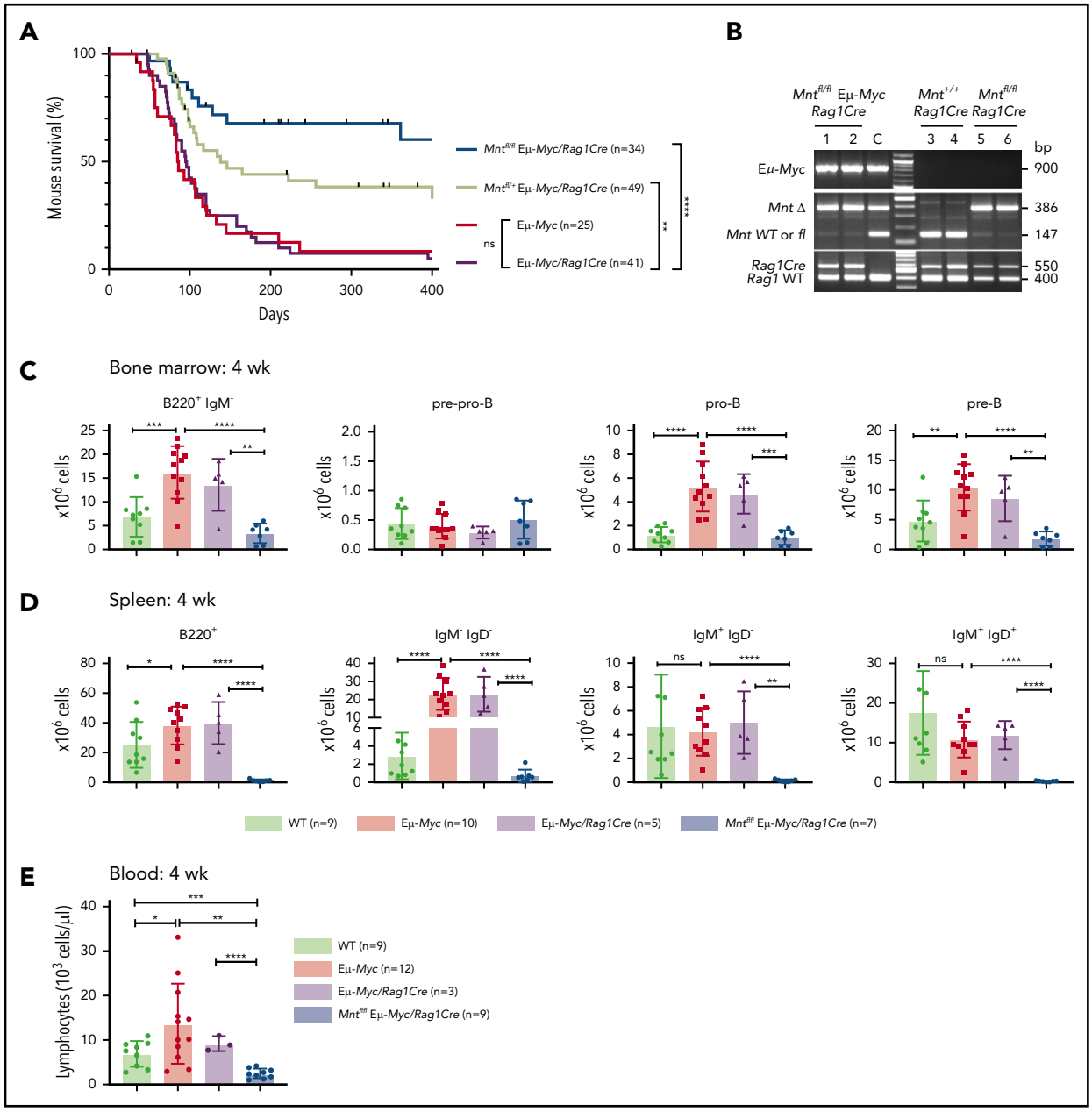

Figure 1. Lymphoid-specific loss of MNT greatly diminishes lymphoma development and induces lymphopenia in Eμ-*Myc* mice. (A) Kaplan-Meier survival curves showing reduced lymphoma development in *Mnt*$^{fl/fl}$ Eμ-*Myc/Rag1Cre* mice (blue; median survival, 463 days) than *Mnt*$^{fl/+}$ Eμ-*Myc/Rag1Cre* mice (lime green; median survival, 138 days) and control Eμ-*Myc* mice (red; median survival, 86 days) and Eμ-*Myc/Rag1Cre* mice (purple; median survival, 96 days). $^{**}P \leq .01$; $^{****}P \leq .0001$. Log-rank test. Killed mice showing no malignancy on autopsy were censored (black mark). X-axis was arbitrarily terminated at 400 days, but monitoring continued. (B) PCR analysis shows efficient deletion of floxed *Mnt* alleles by *Rag1Cre* in cells sorted from bone marrow of individual 4-week-old mice. WT and floxed *Mnt* alleles both produce 147-bp fragments, deleted Mnt allele (*Mnt*Δ), a 386-bp fragment. Lanes 1,2: pro-B and pre-B cells, respectively, from *Mnt*$^{fl/fl}$ Eμ-*Myc/Rag1Cre* mouse #360; lanes 3,4: pre-B cells from control *Mnt*$^{+/+}$ *Rag1Cre* mice (#403, #404); lanes 5,6 pre-B cells from *Mnt*$^{fl/fl}$ *Rag1Cre* mice (#413, #414); C, control DNA for *Mnt* PCRs. (C-D) Lymphoid-specific MNT loss induces lymphopenia. Flow cytometric quantification of B lymphoid subpopulations in bone marrow (C) and spleen (D) of 4-week-old WT (light green), Eμ-*Myc* (red), Eμ-*Myc/Rag1Cre* (purple), and *Mnt*$^{fl/fl}$ Eμ-*Myc/Rag1Cre* (blue) mice. Supplemental Figure 3A exemplifies sorting strategy. Bar graphs show mean ± SD; $^{*}P \leq .05$; $^{**}P \leq .01$; $^{***}P \leq .001$; $^{****}P \leq .0001$. (E) Lymphocyte count in blood of 4-week-old mice of indicated genotypes, determined in an Advia hematology analyzer. Mean ± SD; $^{*}P \leq .05$; $^{**}P \leq .01$; $^{***}P \leq .001$; $^{****}P \leq .0001$.

(B220$^+$IgM$^-$IgD$^-$), immature B (B220$^+$IgM$^+$IgD$^-$) and mature follicular B (B220$^+$IgM$^+$IgD$^+$). Circulating lymphocytes, normally elevated in young Eμ-*Myc* mice, were even lower in *Mnt*-deficient Eμ-*Myc* mice than in WT mice (Figure 1E).

Unsurprisingly, *Mnt*$^{fl/+}$ Eμ-*Myc/Rag1*Cre mice had a milder preleukemic phenotype than *Mnt*$^{fl/fl}$ Eμ-*Myc/Rag1*Cre mice: B lymphoid cells were not significantly diminished in the bone marrow, but the spleen had a significant reduction (~2-fold), and blood lymphocytes were also low (supplemental Figure 3B).

Mnt deletion mediated by *CreERT2* also produces B lymphopenia

To confirm these results in an acute model of *Mnt* deficiency, we used the *Rosa26.CreERT2* transgene (hereafter *CreERT2*), which encodes Cre recombinase fused to a modified hormone-binding

domain of the estrogen receptor within the *Rosa26* locus.[36] Five-week-old *Mnt*$^{fl/fl}$ Eμ-*Myc/CreERT2* and control Eμ-*Myc* and Eμ-*Myc/CreERT2* mice were treated on 3 successive days with tamoxifen by oral gavage and analyzed 4 weeks later (supplemental Figure 4A), to avoid early transient tamoxifen toxicity.[41] PCR and immunoblot analyses of CD19$^+$ splenocytes demonstrated highly efficient deletion of floxed *Mnt* alleles and barely detectable MNT protein in 5 independent experiments (eg, supplemental Figure 4B-C).

The bone marrow of tamoxifen-treated *Mnt*$^{fl/fl}$ Eμ-*Myc/CreERT2* mice had a significant deficit (2- to 3-fold) of B220$^+$IgM$^-$ cells (supplemental Figure 4D). Although pre-pro-B cells were unaffected, both pro-B cells and pre-B cells were substantially reduced (~3-fold) and splenic B lymphoid cells (B220$^+$) were severely depleted (~5-fold; supplemental Figure 4E).

Thus, MNT loss engineered by 2 independent approaches abrogated the MYC-driven lymphocyte expansion that normally hallmarks young Eμ-*Myc* mice. The reduced pool of proliferating premalignant early B lineage cells was undoubtedly a major contributing factor to the reduced lymphoma incidence in MNT-deficient Eμ-*Myc* mice.

MNT loss exacerbates Eμ-*Myc*-driven apoptosis

To identify the mechanism for the profound decrease in B lymphoid cells in young MNT-deficient Eμ-*Myc* mice, we analyzed MYC levels, cell proliferation, senescence, and apoptosis in pro-B and pre-B cells from the bone marrow of 4-week-old *Mnt*$^{fl/fl}$ Eμ-*Myc/Rag1Cre* and control mice. MYC protein was substantially higher in Eμ-*Myc* pro-B and pre-B cells than in WT cells, as expected, but its level did not differ significantly between Eμ-*Myc* cells that had or lacked MNT (Figure 2A). Cell cycle analysis of bone marrow cells (Figure 2B) indicated that MNT loss did not diminish Eμ-*Myc*-driven cycling of pre-B cells,[27] although pro-B cell cycling appeared marginally suppressed. The proportion of senescent cells was comparable in pro-B cells of all 3 genotypes, as measured by intracellular staining for H3K9 trimethylation,[42] and although a small, non-significant increase was noted in pre-B cells expressing Eμ-*Myc*, MNT loss had no effect (Figure 2C).

Notably, however, MNT loss significantly exacerbated apoptosis of Eμ-*Myc* B lymphoid cells (Figure 2D). Annexin-V$^+$ cells in bone marrow pro-B and pre-B cell populations of MNT-deficient Eμ-*Myc* mice (blue) were ~3-fold higher than for regular Eμ-*Myc* mice (red), which in turn were ~3-fold higher than for cells from WT mice (light green).

MNT loss increases apoptosis in situ in bone marrow

To complement these ex vivo analyses, we immunostained non-decalcified long bones[38,39,43] from 4-week-old (premalignant) Eμ-*Myc* mice of all genotypes for CD19 (B lymphoid cells), Ki67 (proliferation), and cleaved caspase-3 (apoptosis) and collected a tilescan map by dual 2-photon/confocal microscopy. Representative stained images are presented in Figure 3A-B, and whole-bone staining is quantified in Figure 3C-E. The bones from Eμ-*Myc* and Eμ-*Myc/Rag1Cre* mice were packed with CD19$^+$ and Ki67$^+$ cells, as anticipated. In contrast, *Mnt*-deleted Eμ-*Myc* mice (*Mnt*$^{fl/fl}$ Eμ-*Myc/Rag1Cre*) had far fewer CD19$^+$ cells, consistent with analysis by flow cytometry (Figure 1C). The low level of Ki67-positive cells in bones isolated from *Mnt*$^{fl/fl}$ Eμ-*Myc/Rag1Cre* mice undoubtedly reflects this B lymphopenia. Of note, cleaved caspase-3-positive cells were as prevalent in *Mnt*$^{fl/fl}$ Eμ-*Myc/Rag1Cre* bones as in those from Eμ-*Myc* and Eμ-*Myc/Rag1Cre* mice (Figure 3E), consistent with a higher proportion of the B lymphoid cells being apoptotic.

Taken together, these ex vivo (Figure 2) and in situ (Figure 3) analyses strongly suggest that increased apoptosis is the dominant effect of MNT loss during B lineage development in Eμ-*Myc* mice.

MNT loss also constrains B lymphoid development in WT mice

Because induction of apoptosis by MYC depends on its level of expression,[7] whether MNT deficiency would affect normal B lymphopoiesis was unclear. To assess this, we compared B lymphoid cell subpopulations in 6-week-old WT, *Rag1Cre*, and *Mnt*$^{fl/fl}$ *Rag1Cre* mice (exemplified in supplemental Figure 5). Notably, *Mnt* deletion significantly reduced B lymphoid cell numbers in both the bone marrow and spleen, although the reduction was less pronounced than in Eμ-*Myc* mice (Figure 4A-B). Tamoxifen-treated *Mnt*$^{fl/fl}$*CreERT2* mice also developed B lymphopenia, having fewer pre-pro-B, pro-B, pre-B, and B cells (Figure 4C-D). Thus, MNT loss impairs normal as well as Eμ-*Myc*-driven B lymphopoiesis.

MNT constrains B lymphoid apoptosis largely by down-regulating expression of pro-apoptotic BIM

B lymphopoiesis in the bone marrow depends on signaling through the interleukin 7 (IL-7) receptor.[44] Hence, to explore the mechanism underlying the enhanced apoptosis of MNT-deficient but otherwise normal B lymphoid cells, we cultured bone marrow-derived B progenitor cells (CD19$^+$IgM$^-$) in IL-7. In WT cells, endogenous MYC protein increased substantially by 48 hours, and MNT and anti-apoptotic MCL-1 also rose (Figure 5A). MNT deficiency had little effect on either the MYC level (supplemental Figure 6A) or the proliferation profile (supplemental Figure 6B) of pro-B cells cultured for 4 days in IL-7. Strikingly, however, apoptotic pro-B cells (annexin-V+) increased ~3-fold (Figure 5B,E), despite the supraoptimal levels of IL-7.

BIM, a potent BH3-only protein in the BCL-2 family,[32,33] is a major apoptotic trigger during B lymphopoiesis.[45-47] Flow cytometry and immunoblotting (Figure 5C-D) revealed higher BIM protein in cultured pro-B cells from *Mnt*$^{fl/fl}$ *Rag1Cre* mice than in their WT counterparts, although *Bim* mRNA was unchanged (supplemental Figure 6D). MCL-1 protein (and RNA) levels fell in MNT-deficient pro-B cells (Figure 5D; supplemental Figure 6D), which would also increase susceptibility to apoptosis.

As BIM expression is haploinsufficient,[31,45] we tested whether loss of a single *Bim* allele could ameliorate the pro-apoptotic effect of MNT loss. Indeed, the proportion of apoptotic pro-B cells in day 4 IL-7 cultures of *Bim*$^{+/-}$ *Mnt*$^{fl/fl}$ *Rag1Cre* cells (light orange) was significantly lower than for *Mnt*$^{fl/fl}$ *Rag1Cre* cells (light blue; Figure 5E). *Bim* heterozygosity did not, however, rescue the lower MCL-1 in IL-7 cultured pro-B cells lacking MNT (supplemental Figure 6C).

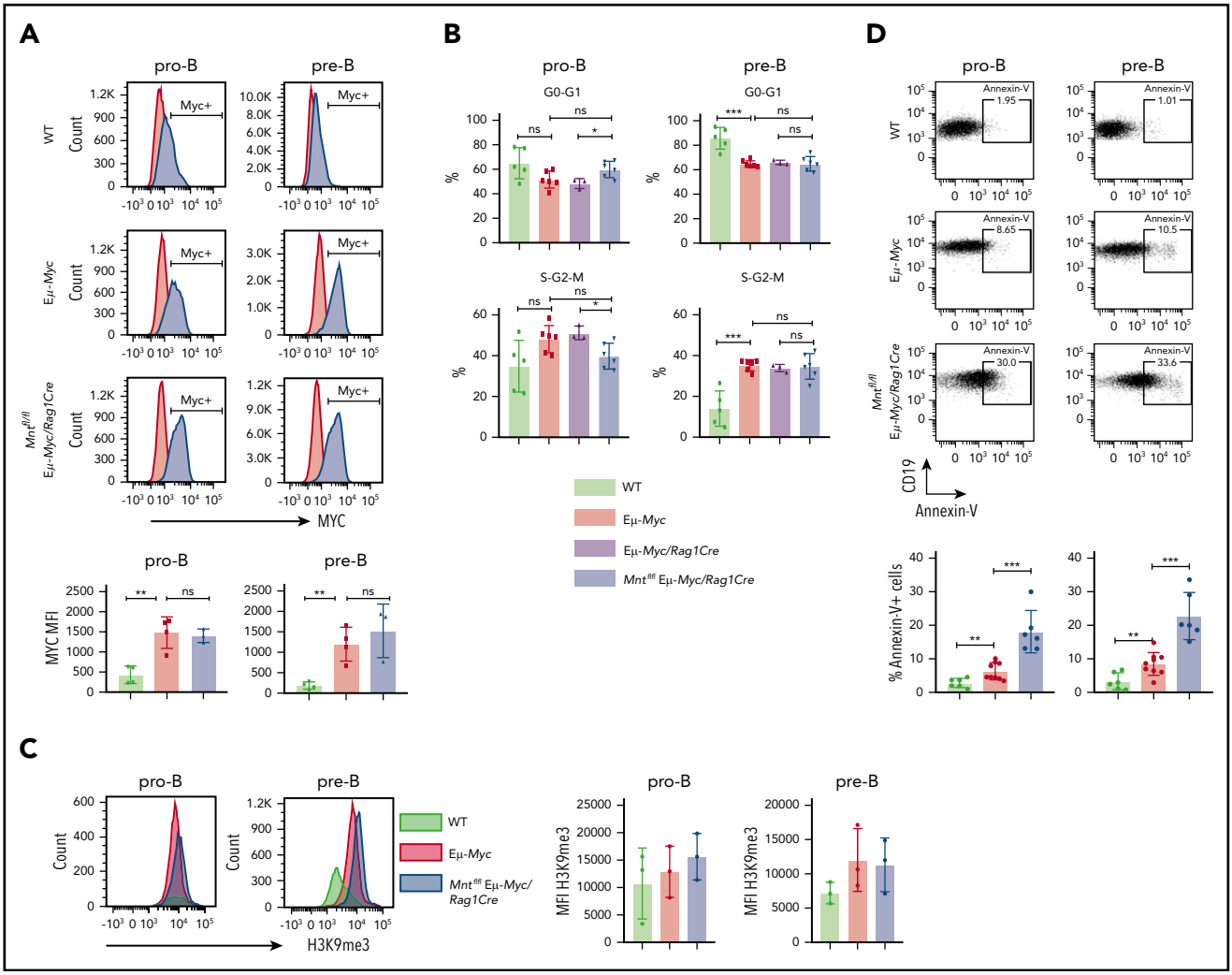

Figure 2. *Mnt* deletion increases apoptosis but does not affect MYC protein level, cell cycling, or senescence in premalignant Eμ-*Myc* pro-B and pre-B cells. (A) MNT loss does not change MYC level. Pro-B and pre-B cells were sorted from bone marrow of 4-week-old mice, permeabilized and stained with MYC antibody (blue) or isotype-matched control (red). (Bottom) Mean intracellular MYC fluorescence (MFI) ± SD in WT (light green), Eμ-*Myc* (red), and *Mnt*$^{fl/fl}$ Eμ-*Myc/Rag1Cre* (blue) pro-B and pre-B cells; n = 3 or 4; mean ± SD; $^{**}P \leq .01$; ns = not significant. (B) Cell cycle analysis. DNA content of 4′,6-diamidino-2-phenylindole-stained cells shows that the proportion of cycling (S-G2-M) pre-B cells in *Mnt*$^{fl/fl}$ Eμ-*Myc/Rag1Cre* (blue) is comparable to that in Eμ-*Myc* (red) and Eμ-*Myc/Rag1Cre* (purple) mice. n = 3-6. Mean ± SD; $^{*}P \leq .05$; $^{**}P \leq .01$. (C) MNT loss does not significantly affect H3K9 trimethylation. Representative H3K9me3 staining of sorted permeabilized pro-B and pre-B cells from 4-week WT (light green), Eμ-*Myc* (red), and *Mnt*$^{fl/fl}$ Eμ-*Myc/Rag1Cre* (blue) mice (left panels) and MFI for 3 mice of each genotype in 3 independent experiments (right panels). (D) MNT loss markedly elevates apoptosis. Annexin-V+ pro-B and pre-B cells were 2- to 3-fold more frequent in bone marrow of Eμ-*Myc* (red) than WT (light green) mice and ~3-fold higher in *Mnt*$^{fl/fl}$ Eμ-*Myc/Rag1Cre* (blue) than in Eμ-*Myc* mice. Top panels show typical fluorescence-activated cell sorting plots, and bottom panel shows mean percentage annexin-V^{+} cells; n = 6 to 9 individual mice; mean ± SD; $^{**}P \leq .01$; $^{***}P \leq .001$.

Taken together, these studies show that IL-7 receptor signaling upregulates MNT as well as MYC, and suggest that MNT reduces the MYC-induced apoptotic response, thereby facilitating MYC-driven cell production. They also suggest that the increased apoptosis of MNT-deficient pro-B cells is a result of elevated BIM levels, and probably also lower MCL-1.

Loss of a single *Bim* allele abrogates B lymphopenia provoked by MNT loss

These in vitro findings made it likely that the B lymphopenia induced in WT and Eμ-*Myc* mice by MNT loss reflected, at least in part, BIM-mediated apoptosis. Accordingly, MNT-deficient CD19^{+} spleen cells had more BIM protein than WT cells (compare lane 1 and 2 in Figure 6A), and BIM was even higher in splenocytes from Eμ-*Myc* mice (lane 4).

We therefore tested whether *Bim* heterozygosity would ameliorate B lymphopenia in MNT-deficient mice. Indeed, lowering BIM partially restored B220^{+} cell numbers in the bone marrow of young *Mnt*$^{fl/fl}$ *Rag1Cre* mice (Figure 6B), and even more so in their spleen (Figure 6C) (compare light orange and light blue bars).

Bim heterozygosity also significantly ameliorated the B lymphopenia provoked by MNT loss in young Eμ-*Myc* mice. Total B lymphoid cells in the bone marrow (Figure 6D) and spleen (Figure 6E) of *Bim*$^{+/-}$ MNT-deficient Eμ-*Myc* mice were significantly more frequent than in *Bim*$^{+/+}$ MNT-deficient Eμ-*Myc* mice (compare orange with blue bars), primarily as a result of more pro-B and pre-B cells. Annexin V staining of bone marrow pro-B and pre-B cells (Figure 6F) confirmed that *Bim* heterozygosity (orange) significantly reduced apoptosis of

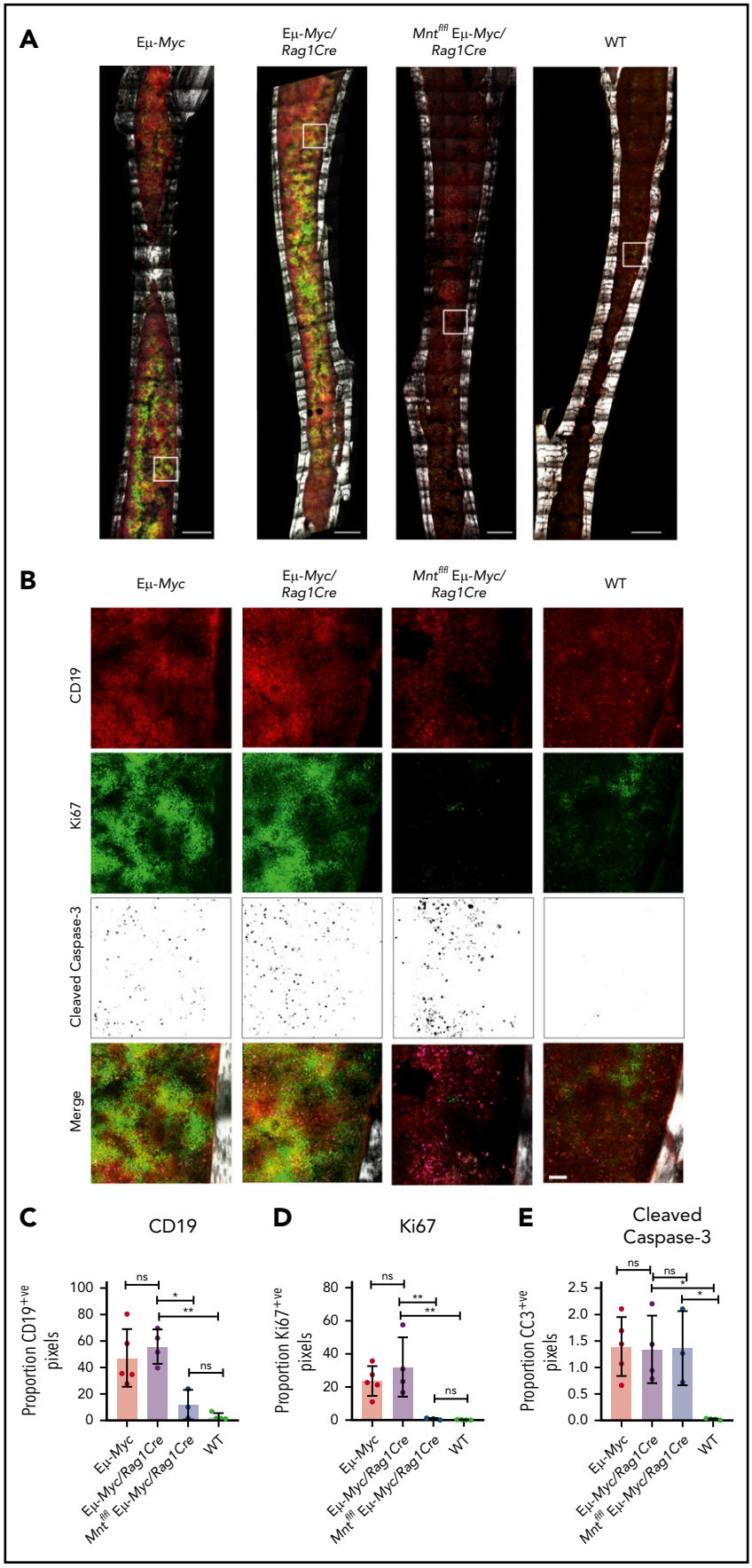

Figure 3. In situ analysis of cell proliferation and apoptosis. (A) Tilescan sections of whole tibia. Bones were harvested from 4-week old Eμ-*Myc* (n = 5), Eμ-*Myc/Rag1Cre* (n = 4), *Mnt*$^{fl/fl}$ Eμ-*Myc/Rag1Cre* (n = 3), and WT (n = 4) mice, stained and imaged by combined 2-photon/confocal imaging of cell populations *in situ*. Red = CD19; green = Ki67; magenta = cleaved caspase-3; gray = second harmonic generation (bone). To better visualize CC3-positive cells in Figure 3B, the data are presented using an inverse black and white LUT (Lookup Table). Scale bar, 500 μm. (B) Zoomed areas from original tilescans in panel A (white boxes) with individual channels for CD19, Ki67, and cleaved caspase-3. A merged image (bottom panel) from each area is shown relative to bone signal (gray). Scale bar, 50 μm. (C-E) Quantification of cells in tibia positive for CD19, Ki67, and cleaved caspase-3. Color images were separated into single binary channels and then thresholded, and the number of positive pixels for each whole bone section quantified for CD19 (C), Ki67 (D) and cleaved caspase-3 (E). Each data point represents a whole quantified bone from an individual mouse in each genotype (n = 3-5). Bar graphs show mean ± SD; significance was determined by analysis of variance $^*P \leq .05$; $^{**}P \leq .01$).

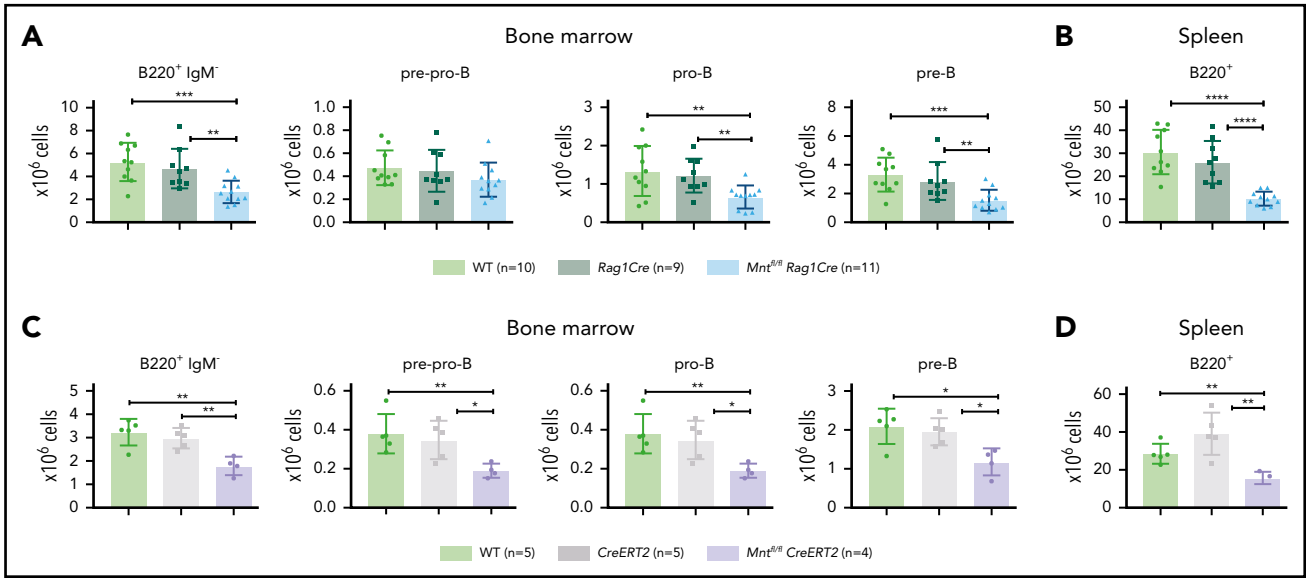

Figure 4. Loss of MNT impedes normal B lymphoid development. (A-B) Deletion of floxed *Mnt* by *Rag1Cre* provokes lymphopenia in mice lacking Eμ-*Myc* transgene. Quantification of B lymphoid subpopulations from bone marrow (A) and spleen (B) of 4-week-old WT (light green), *Rag1Cre* (green), and $Mnt^{fl/fl}$ *Rag1Cre* (light blue) mice. Supplemental Figure 5A exemplifies sorting strategy. n indicates number of mice. Mean ± SD; $^{**}P \leq .01$; $^{***}P \leq .001$; $^{****}P \leq .0001$. (C-D) Activation of CreERT2 by tamoxifen also provokes B lymphopenia in mice lacking Eμ-*Myc* transgene. Quantification of indicated B lymphoid populations from bone marrow (C) and spleen (D). Young (6-week-old) WT (light green), *CreERT2* (gray), and $Mnt^{fl/fl}$ *CreERT2* (lavender) mice were treated for 3 days with tamoxifen by oral gavage and analyzed 4 weeks later. n indicates number of mice. Bar graphs show mean ± SD; $^{*}P \leq .05$; $^{**}P \leq .01$.

$Mnt^{fl/fl}$ Eμ-*Myc/Rag1Cre* pro-B and pre-B cells (compare orange with blue bars).

Most strikingly, Figure 6G shows that the extended tumor-free survival afforded to Eμ-*Myc* mice by homozygous (blue) or even heterozygous *Mnt* (lime green) loss was greatly diminished by concomitant heterozygous loss of *Bim* (compare blue with orange curve and lime green with mustard curve). These observations raised the possibility that the MNT-deficient tumors arising at low frequency in $Mnt^{fl/fl}$ Eμ-*Myc/Rag1Cre* mice might have suffered mutations or epigenetic changes that reduce BIM levels. Indeed, most of these tumors (10 of 13) did have markedly less BIM (supplemental Figure 1C; supplemental Table 1).

Eμ-*Myc* tumor cells remain dependent on MNT to curb MYC-induced apoptosis

Thus far, our results have shown that MNT plays a vital anti-apoptotic role during early B lymphopoiesis, most strongly in Eμ-*Myc*, but also in WT, mice. We hypothesized, therefore, that the survival of fully malignant Eμ-*Myc* lymphoma cells might still require MNT. To test this, we exploited our $Mnt^{fl/fl}$ Eμ-*Myc/CreERT2* mice, which develop Eμ-*Myc* lymphomas carrying tamoxifen-deletable *Mnt* alleles (Figure 7A).

We first tested 2 short-term cell lines derived from independent primary $Mnt^{fl/fl}$ Eμ-*Myc/CreERT2* lymphomas. In both lines, exposure to 4-OH tamoxifen for 24 hours greatly reduced MNT levels, and annexin-V^+ cells were ~3-fold higher than in a control $Mnt^{+/+}$ Eμ-*Myc/CreERT2* line (Figure 7B). Thus, fully transformed Eμ-*Myc*-driven lymphoma cells depend on MNT for survival in vitro.

As a more stringent test, we induced *Mnt* deletion in vivo in transplanted primary lymphoma cells, predicting that MNT loss would disadvantage the tumor cells and hence prolong survival of transplant recipients. Fourteen independent $Mnt^{fl/fl}$ Eμ-*Myc/CreERT2* lymphomas and 9 independent $Mnt^{+/+}$ Eμ-*Myc/CreERT2* control lymphomas were transplanted into nonirradiated syngeneic mice (6 recipient mice per lymphoma), and once the lymphoma cells were established (5 days), 3 of the 6 recipients were treated with tamoxifen and 3 with vehicle alone. As expected, tamoxifen provided no survival benefit to recipients of control (Eμ-*Myc/CreERT2*) lymphoma cells (Figure 7C, lower panel). In marked contrast, after tamoxifen treatment, mice bearing $Mnt^{fl/fl}$ Eμ-*Myc/CreERT2* lymphoma cells survived significantly longer (Figure 7C, upper panel; $P < .0001$), whether transplanted with IgM^+ or with IgM^- tumors (supplemental Figure 7A). Comparable experiments with $Mnt^{+/-}$ Eμ-*Myc/CreERT2* lymphomas showed that tamoxifen-induced loss of even a single *Mnt* allele significantly extended recipient survival (supplemental Figure 7B).

Strikingly, for 2 of the $Mnt^{fl/fl}$ Eμ-*Myc/CreERT2* tumors (#508 and #874), all (6/6) tamoxifen-treated transplant recipients survived for more than 19 weeks and were deemed "cured" (all their vehicle-treated recipients had required euthanasia within ~30 days). Eleven other tumors had a median survival benefit of 8.3 days (range, 4-22 days), and 1 had none (supplemental Table 2). To address why the response rate varied, we analyzed $CD19^+$ $Ly5.2^+$ cells isolated by fluorescence-activated cell sorting from relapsing $Mnt^{fl/fl}$ Eμ-*Myc/CreERT2* lymphomas, comparing those treated with vehicle (as a surrogate for the primary tumor) and those treated with tamoxifen (supplemental Table 2; supplemental Figure 7C-D). For the nonresponding tumor (#676), PCR analysis indicated that failed *Mnt* deletion was a result of loss of the *CreERT2* gene during tamoxifen treatment. The 11 other tumors analyzed retained readily detectable Mnt^{fl} DNA after treatment and still expressed significant MNT protein, suggesting they derived from cells that had escaped complete

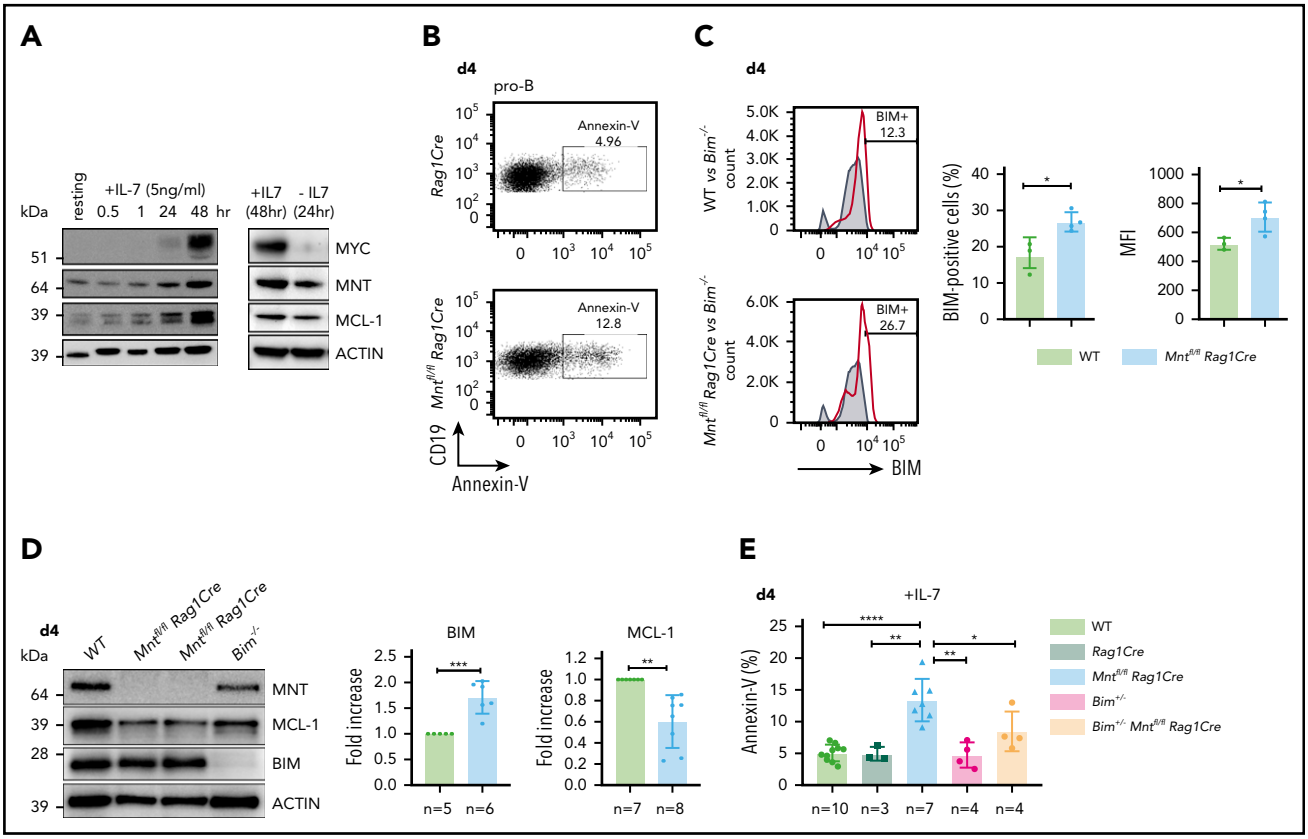

Figure 5. Loss of MNT increases apoptosis of pro-B cells in IL-7 cultures. (A) Expression of MYC, MNT, and MCL-1 protein in CD19^{+}IgM^{-} cells sorted by FACS from bone marrow of 6-week-old WT mice, before and during culture in IL-7, and 24 hours after IL-7 removal. (B-D) MNT-deficient pro-B cells exhibit increased apoptosis, elevated BIM, and decreased MCL-1. Pro-B cells were obtained by culturing CD19^{+} bone marrow cells (isolated using microbeads) in IL-7 (5 ng/ml) for 4 days. (B) Annexin-V staining of *Rag1Cre* and *Mnt*$^{fl/fl}$ *Rag1Cre* pro-B cells; profiles are typical of those from ≥3 mice of each genotype (see panel E). (C) Flow cytometric analysis of intracellular BIM using *Bim*$^{-/-}$ cells (gray shaded) as a negative control. Bar graphs compare percentage BIM-positive cells and mean fluorescence intensity (MFI) from WT (light green) vs *Mnt*$^{fl/fl}$ *Rag1Cre* (light blue) mice, determined in 3 independent experiments; MFI of BIM-null cells was subtracted from that of either WT or *Mnt*$^{fl/fl}$ *Rag1Cre* cells stained in same experiment. (D) Typical western blot of pro-B cells from WT, *Mnt*$^{fl/fl}$ *Rag1Cre* and control *Bim*$^{-/-}$ mice. For each blot, BIM and MCL-1 levels were quantified relative to ACTIN and normalized to WT value. Bar graphs show mean fold-change ± SD $^{**}P \leq .01$; $^{***}P \leq .001$. (E) *Bim* heterozygosity significantly reduces apoptosis of MNT-null pro-B cells. Cells were stained with annexin-V after 4 days in IL-7. Bar graphs show mean ± SD; $^{*}P \leq 0.05$; $^{**}P \leq .01$; $^{****}P \leq .0001$.

Mnt deletion. Thus, Figure 7C likely underestimates the true effect of MNT loss.

As 4/14 (29%) transplanted *Mnt*$^{fl/fl}$ Eμ-*Myc/CreERT2* lymphomas (including #508) lacked functional p53 (supplemental Figure 7D; supplemental Table 2), vulnerability to MNT loss did not appear to rely on WT p53. To directly test this, we established cell lines from independent primary *Mnt*$^{fl/fl}$ Eμ-*Myc/CreERT2* lymphomas and ascertained their p53 status by exposure to nutlin 3a[48] (supplemental Figure 8). Figure 7D shows that 4/4 p53 WT *Mnt*$^{fl/fl}$ Eμ-*Myc/CreERT2* lines were extremely sensitive to apoptosis after *Mnt* deletion, and that 4/4 p53 mutant *Mnt*$^{fl/fl}$ Eμ-*Myc/CreERT2* lines were also vulnerable, albeit to a lesser degree.

Discussion

The proliferation of lymphocytes, similar to most cell types, requires MYC.[49] MYC's proliferative drive is checked, however, by its propensity to induce apoptosis at high expression levels.[7] In this study, using conditional deletion in normal and Eμ-*Myc* mice, we provide strong genetic evidence that MYC antagonist MNT plays a vital role in both normal B lymphopoiesis and MYC-driven lymphomagenesis by reducing MYC-driven apoptosis. These results have important implications for the treatment of lymphomas and potentially other MYC-driven tumor types.

MNT was detectable at each major stage of B-cell development in the marrow of young WT mice, the highest levels being in pre-B and IgM^{+} B cells (supplemental Figure 2). Of note, MNT levels in Eμ-*Myc* mice were ~3-fold higher than in comparable populations from WT mice.

Strikingly, homozygous deletion of floxed *Mnt* alleles in early B-cell progenitors (via *Rag-1Cre*) significantly extended the lifespan of Eμ-*Myc* mice by reducing the overall incidence of lymphomas (from >90% to ~35%) and retarding their development (Figure 1A). The reduced lymphomagenesis in *Mnt*$^{fl/fl}$ Eμ-*Myc/Rag1Cre* mice correlated with a profound early depletion of proliferating premalignant pro-B and pre-B cells (Figure 1C-E), the cells at risk of acquiring the oncogenic mutations needed for fully fledged malignancy.[28] Enhanced apoptosis proved to be the major cause of this deficit, rather than reduced proliferation or increased cellular senescence (Figures 2 and 3). We conclude that MNT plays a major role in suppressing apoptosis driven by the high MYC levels in B lymphoid cells of Eμ-*Myc* mice.

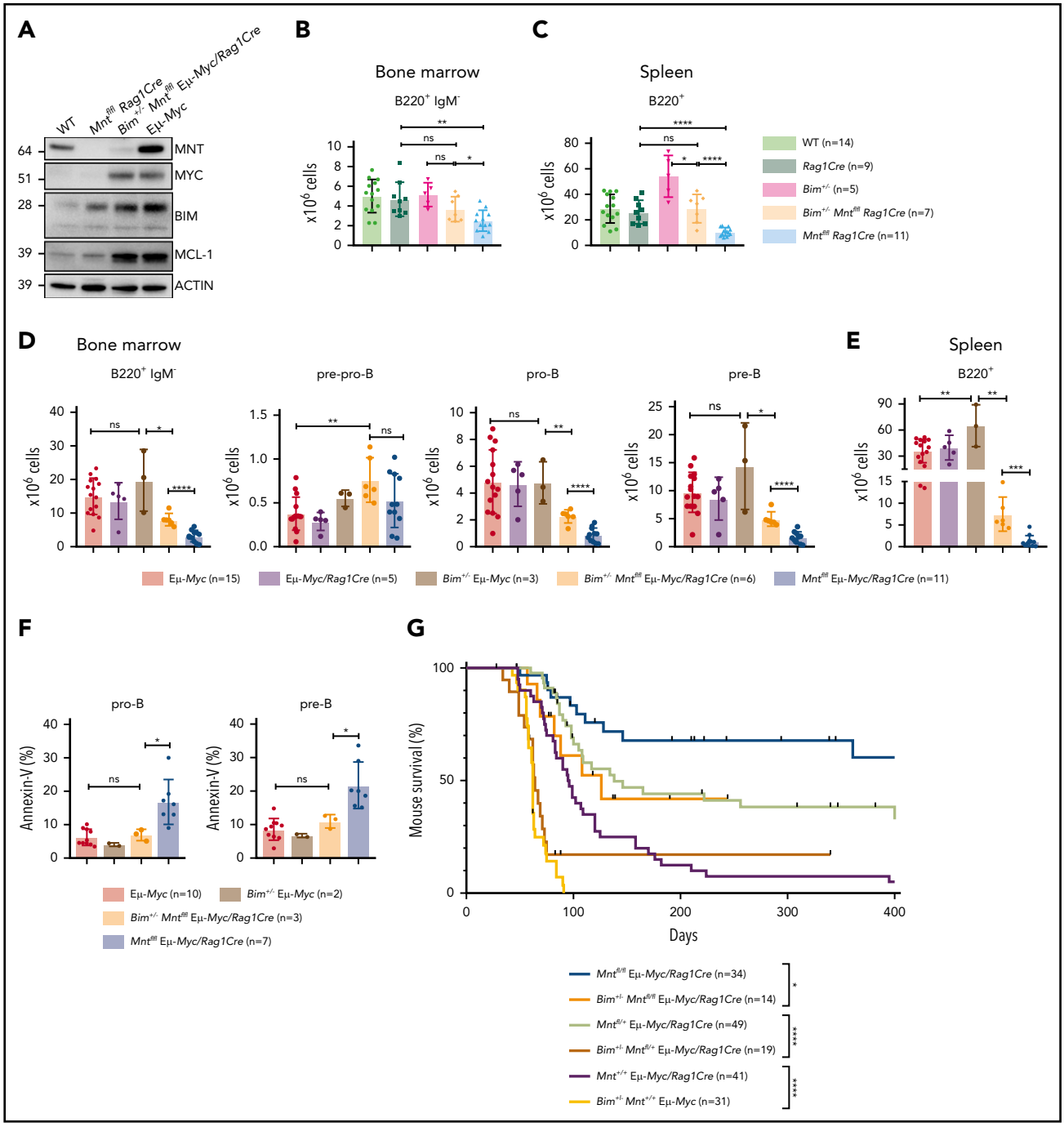

Figure 6. *Bim* heterozygosity rescues B lymphopoiesis, reduces apoptosis, and accelerates lymphomagenesis in MNT-deficient Eμ-*Myc* mice. (A) BIM and MCL-1 expression is elevated in MNT-deficient CD19$^+$ cells. Cells were fluorescence-activated cell sorted from spleens of 4-week-old mice. (B-C) *Bim* heterozygosity largely restores B lymphopoiesis in young *Mnt*$^{fl/fl}$ *Rag1Cre* mice. Flow cytometric enumeration of B lymphoid cells in bone marrow (B) and spleen (C) of 6-week-old mice. Data include mice in Figure 4 plus additional mice. Bar graphs show mean ± SD; *$P \leq .05$; **$P \leq .01$; ****$P \leq .0001$. (D-E) *Bim* heterozygosity partially restores B lymphopoiesis in young MNT-deficient Eμ-*Myc* mice. Enumeration of B lymphoid cell populations in (D) bone marrow and (E) spleen of the indicated genotypes. Data for controls include certain mice in Figure 1C-D. Mean ± SD; *$P \leq .05$; **$P \leq .01$; ****$P \leq .001$; ****$P \leq .0001$. (F) *Bim* heterozygosity ameliorates enhanced apoptosis of pro-B and pre-B cells in the bone marrow of young MNT-deficient Eμ-*Myc* mice. Data include mice from Fig. 1C. Mean ± SD; *$P \leq .05$; ns = not significant. (G) *Bim* heterozygosity accelerates lymphomagenesis in MNT-deficient Eμ-*Myc* mice. Kaplan-Meier survival curves showing enhanced morbidity of *Bim*$^{+/-}$ *Mnt*$^{fl/fl}$ Eμ-*Myc/Rag1Cre* (orange) mice compared with *Mnt*$^{fl/fl}$ Eμ-*Myc/Rag1Cre* (blue) mice, and of *Bim*$^{+/-}$ *Mnt*$^{fl/+}$ Eμ-*Myc/Rag1Cre* (mustard) mice compared with *Mnt*$^{fl/+}$ Eμ-*Myc/Rag1Cre* (lime green) mice. Survival curves for Eμ-*Myc/Rag1Cre*, *Mnt*$^{fl/+}$ Eμ-*Myc/Rag1Cre*, and *Mnt*$^{fl/fl}$ Eμ-*Myc/Rag1Cre* mice are those shown in Figure 1A. Log-rank test; *$P \leq .05$; ****$P \leq .0001$.

Mnt deletion also reduced B lymphoid cell numbers in the bone marrow and spleen of normal mice (Figure 4), although the cell deficit was less than in Eμ-*Myc* mice. Thus, normal B-cell development also depends on MNT, perhaps because endogenous MYC levels can rise above the proapoptotic threshold at certain stages during their ontogeny. The most vulnerable population is likely to be the highly proliferative pro-B cell stage, in which MYC expression is highest

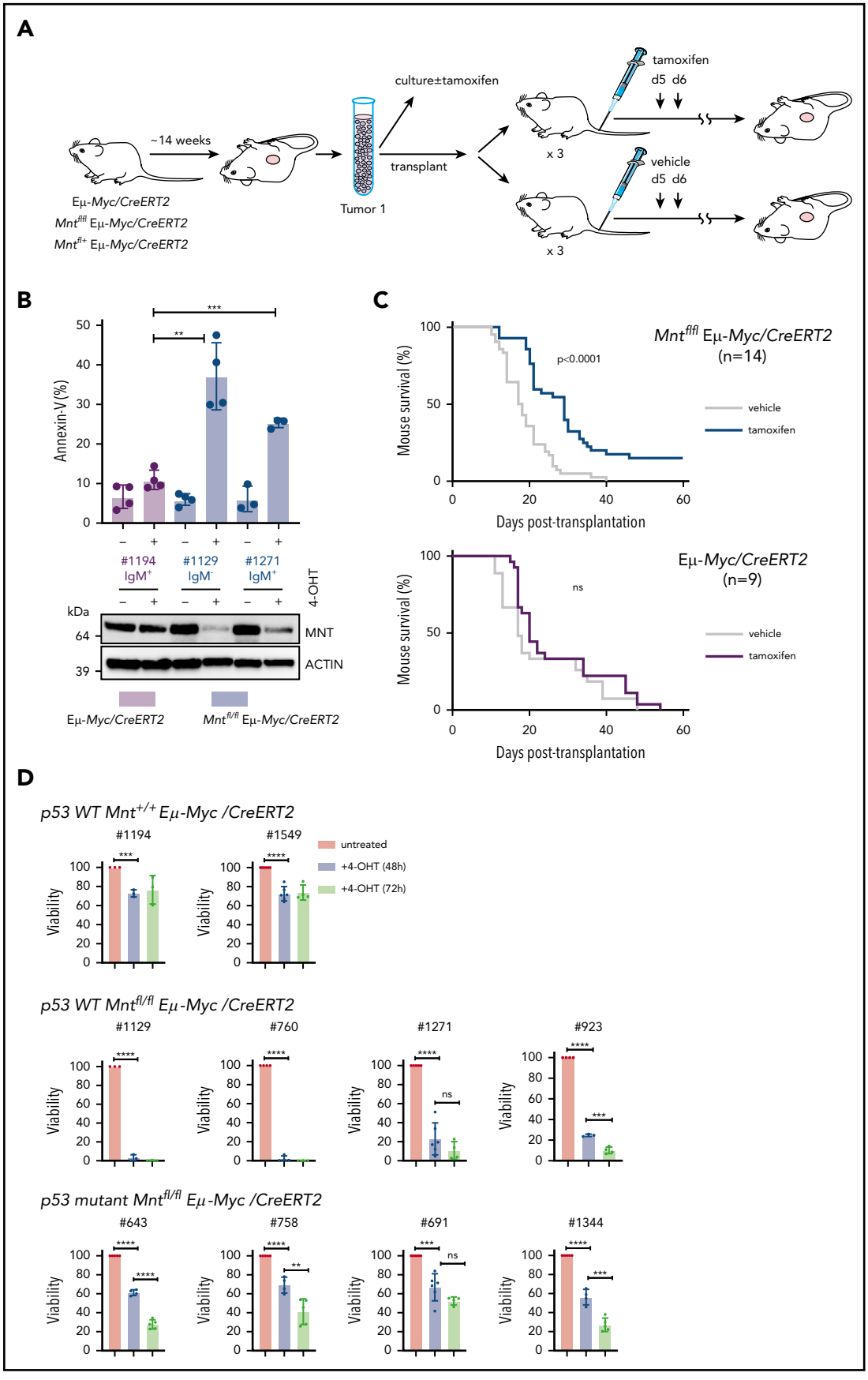

Figure 7.

(Figure 2A; see also the immgen.org database and Huang et al[50]), and which is dependent on IL-7 for proliferation and survival.[51]

These investigations of MNT function confirm and greatly extend previous genetic studies.[25,26] Link et al reported that T lymphoid-specific *Mnt* deletion prevented thymic lymphoma development in transgenic mice expressing a mutant, more stable form of MYC, and that thymocytes lacking MNT were more susceptible to apoptosis.[25] Our own previous study,[26] using mice constitutively heterozygous for *Mnt*,[37] found retarded lymphomagenesis in Eμ-*Myc* and VavP-*MYC10* mice. However, there was no measurable enhancement of apoptosis in $Mnt^{+/-}$ Eμ-*Myc* B lymphoid cells. This disparity with our current findings undoubtedly reflects the greater effect of homozygous vs heterozygous loss of *Mnt* (compare Figure 1 and supplemental Figure 3B), but the germline deletion may also have selected for compensatory mechanisms to overcome developmental disadvantage.

In a major advance, we have established that the BH3-only protein BIM, a potent proapoptotic BCL-2 family member,[32,33] is in part responsible for the increased apoptosis of MNT-deficient MYC-driven B lymphoid cells (Figure 6). BIM protein levels were higher in MNT-deficient pro-B cells (Figure 5C-D), apparently as a result of posttranscriptional mechanisms (supplemental Figure 6D), and tellingly, *Bim* heterozygosity reduced apoptosis of $Mnt^{fl/fl}$ Eμ-*Myc/Rag1Cre* pro-B and pre-B cells (Figure 6F). Furthermore, lymphomas arose significantly faster and more frequently in $Bim^{+/-}$ $Mnt^{fl/fl}$ Eμ-*Myc/Rag1Cre* than in $Bim^{+/+}$ $Mnt^{fl/fl}$ Eμ-*Myc/Rag1Cre* mice (Figure 6G).

Although *Bim* heterozygosity substantially alleviated the B lymphopenia in premalignant MNT-deficient Eμ-*Myc* mice, it did not fully restore cell numbers (Figure 6 D-E). We speculate that lower MCL-1, as observed in cultured MNT-deficient pro-B cells (Figure 5D), may also have contributed to the enhanced apoptosis of MNT-deficient Eμ-*Myc* B lymphoid cells. Pertinently, MCL-1 is essential for the development and sustained growth of Eμ-*Myc* lymphoma cells.[52,53]

Another striking advance reported here is that even fully malignant (transplantable) Eμ-*Myc*-driven cells remain MNT-dependent (Figure 7). 4OH-tamoxifen-induction of *Mnt*-deletion in cell lines from $Mnt^{fl/fl}$ Eμ-*Myc/CreERT2* lymphomas rapidly induced cell death in vitro, particularly in lines retaining p53 functionality, but also in those lacking it (Figures 7B,D). Furthermore, when multiple $Mnt^{fl/fl}$ Eμ-*Myc/CreERT2* lymphomas were each transplanted into several immunocompetent syngeneic mice, recipients treated with tamoxifen to induce *Mnt* deletion in the tumor cells uniformly lived longer than those treated with vehicle alone (Figure 7C; $P = .0002$). Indeed, the true survival benefit of MNT loss is likely underestimated by this experiment because relapsing lymphoma cells lacked complete *Mnt* deletion. Conversely, the cures achieved for all recipients of 2 lymphomas likely reflected highly efficient *Mnt* loss.

This study clearly establishes that the proliferative capacity of MYC-driven B lymphocytes and lymphoma cells depends on MNT suppression of apoptosis. Thus, in this cellular setting, *Mnt* is a synergistic oncogene rather than a tumor suppressor, as earlier studies suggested,[20,21,23,24] although MNT might well have a tumor suppressor role in certain cell types or circumstances.

Elevated MYC levels are common in lymphoid and many other malignancies,[3] and often correlate with poor prognosis (eg, Barrans et al[54]). In several tumor models, MYC down-regulation can elicit tumor regression (eg, Felsher and Bishop,[55], Meyer and Penn,[56] and Soucek et al[57]). To date, however, drugs that directly target MYC have largely disappointed in the clinic, probably because reducing MYC leads to reduced MYC-driven apoptosis, and new approaches are urgently needed.[58,59]

Our genetic demonstration that MNT loss is a synthetic lethal vulnerability in MYC-driven lymphomas, even those mutant for p53 (Figure 7D), elevates MNT as an exciting prospect for drug development. We suggest that a therapeutic that inhibits or degrades MNT would serve as a Trojan horse by unleashing the intrinsic potential of MYC-driven lymphoma cells for self-destruction by apoptosis. Assessment of MNT and MYC protein levels in different human tumor types may reveal which malignancies might benefit from MNT inhibitors. A drug that substantially lowers MNT should not only elevate spontaneous apoptosis in MYC-driven tumors but also exacerbate sensitivity to diverse cytotoxic agents. Thus, co-targeting MNT could lift the efficacy of many current cytotoxic therapies, including the emerging BH3 mimetic drugs showing such high potential in blood cell cancers.[33] Although a transcription factor such as MNT is a more challenging drug target than an enzyme, a growing number of epigenetic targets are showing promise,[60] and targeted degradation has exciting potential.[61]

Figure 7. MNT loss induced in vivo in Eμ-*Myc* lymphomas extends survival of transplant recipients. (A) Schematic of experimental design. $Mnt^{fl/fl}$ Eμ-*Myc/CreERT2* and Eμ-*Myc/CreERT2* mice were aged until they developed tumors (~100 days). Tumor cells (Ly5.2+) were harvested and either cultured to establish cell lines for in vitro treatment with 4-OH tamoxifen (4-OHT) (see panel B) or injected intravenously into syngeneic nonirradiated C57BL/6-Ly5.1 mice for in vivo treatment with tamoxifen (see panel C). (B) 4-OH tamoxifen-induced *Mnt* loss enhances apoptosis of Eμ-*Myc* lymphoma cells in vitro. Short-term cell lines established from 2 independent $Mnt^{fl/fl}$ Eμ-*Myc/CreERT2* lymphomas (#1129 and #1271) and a control Eμ-*Myc/CreERT2* lymphoma (#1194) were treated for 24 hours with or without 0.5 μM 4-OH tamoxifen and percentage annexin-V-positive cells determined by flow cytometry. Results are from 4 (#1194, #1129) or 3 (#1271) independent experiments; mean ± SD $^{**}P \leq .01$; $^{**}P \leq .001$. Immunoblot shows MNT and ACTIN protein in cells treated with tamoxifen or vehicle. (C) Tamoxifen-induced *Mnt* deletion significantly extends survival of mice transplanted with $Mnt^{fl/fl}$ Eμ-*Myc/CreERT2* lymphomas. Kaplan-Meier survival curves of mice transplanted with 14 independent $Mnt^{fl/fl}$ Eμ-*Myc/CreERT2* or 9 control Eμ-*Myc/CreERT2* lymphomas and subsequently treated with either tamoxifen or vehicle alone. Each lymphoma was transplanted into 6 nonirradiated C57BL/6 recipients (2-4 × 10^6 cells/mouse), 3 of which were treated by oral gavage with tamoxifen and 3 with vehicle alone, for 2 successive days, starting on day 5; n indicates number of independent lymphomas transplanted. Significance was determined using log-rank test. See also Supplemental Figure 6A. (D) Induced *Mnt* deletion reduces viability of p53 wt and p53 mutant $Mnt^{fl/fl}$ Eμ-*Myc/CreERT2* lymphoma cell lines. Cell lines established from $Mnt^{fl/fl}$ Eμ-*Myc/CreERT2* and control $Mnt^{+/+}$ Eμ-*Myc/CreERT2* lymphomas were incubated with 0.5 μM 4-OH tamoxifen to delete *Mnt*, and cell viability was determined by flow cytometry (supplemental Figure 8). Viability of 4-OHT-treated cells at 48 and 72 hours is expressed relative to that of cells incubated in parallel without 4-OHT. P53 status, determined by treatment with nutlin3a, is indicated.

Acknowledgments

The authors thank Peter Hurlin (Shriner's Hospital for Children) for his kind gift of $Mnt^{fl/+}$ and $Mnt^{+/-}$ mice; our colleagues Jerry Adams, Andreas Strasser, Steve Nutt, Gemma Kelly, and Philippe Bouillet for comments on the manuscript and useful discussions; Andreas Strasser and Lorraine O'Reilly for fluorescent antibodies; Gemma Kelly, Marco Herold, and Kerstin Brinkmann for advice re tamoxifen activation protocol; Krystal Hughes, Crystal Stivala, Cassandra D'Alessandro, and Giovanni Siciliano for mouse husbandry; Simon Monard for assistance with flow cytometry; and Peter Maltezos for preparation of the figures.

This work was supported by grants from the National Health and Medical Research Council (program grant 461221) (S.C.) and the Leukemia & Lymphoma Society (Specialized Center of Research) grant 7001-13 (S.C.), National Health and Medical Research Council project grants GNT1060179 and GNT1122783 (A.P.N.), Leukemia and Lymphoma Society USA 6552-18, National Health and Medical Research Council APP1145442 and an RD Wright Fellowship APP1159488 (E.D.H.), an Australia Postgraduate Award (J.R.), philanthropic support to the Walter and Eliza Hall Institute, and operational infrastructure grants through the Australian Government Independent Research Institute Infrastructure Support Scheme and the Victorian Government Operational Infrastructure Support.

Authorship

Contribution: H.V.N., C.J.V., and M.R.R. performed most of the experiments; A.P.N. performed histological analysis; N.S.A. helped establish crosses; J.R. and E.D.H. performed and analyzed bone marrow imaging; and S.C. conceived the project, wrote the manuscript with input from authors, and secured funding.

Conflict-of-interest disclosure: The authors declare no competing financial interests.

The current affiliation for N.S.A. is Australian Centre for Blood Diseases, Monash University, Melbourne, VIC, Australia.

ORCID profiles: H.V.N., 0000-0001-6974-1630; C.J.V., 0000-0002-8891-8873; A.P.N., 0000-0001-9690-0879; N.S.A., 0000-0003-2093-1403; J.R., 0000-0001-6488-2784; E.D.H., 0000-0002-3686-8261; S.C., 0000-0002-6818-3451.

Correspondence: Suzanne Cory, The Walter and Eliza Hall Institute of Medical Research, 1G Royal Parade, Parkville, VIC 3052, Australia; e-mail: cory@wehi.edu.au.

Footnotes

Submitted 22 August 2019; accepted 23 December 2019; prepublished online on *Blood* First Edition 24 January 2020. DOI 10.1182/blood.2019003014.

*H.V.N. and C.J.V. are joint first authors.

The online version of this article contains a data supplement.

There is a *Blood* Commentary on this article in this issue.

The publication costs of this article were defrayed in part by page charge payment. Therefore, and solely to indicate this fact, this article is hereby marked "advertisement" in accordance with 18 USC section 1734.

REFERENCES

1. Diolaiti D, McFerrin L, Carroll PA, Eisenman RN. Functional interactions among members of the MAX and MLX transcriptional network during oncogenesis. *Biochim Biophys Acta*. 2015;1849(5):484-500.
2. Dang CV. MYC on the path to cancer. *Cell*. 2012;149(1):22-35.
3. Kalkat M, De Melo J, Hickman KA, et al. MYC Deregulation in Primary Human Cancers. *Genes (Basel)*. 2017;8(6):E151.
4. Adams JM, Harris AW, Pinkert CA, et al. The c-myc oncogene driven by immunoglobulin enhancers induces lymphoid malignancy in transgenic mice. *Nature*. 1985;318(6046):533-538.
5. Askew DS, Ashmun RA, Simmons BC, Cleveland JL. Constitutive c-*myc* expression in an IL-3-dependent myeloid cell line suppresses cell cycle arrest and accelerates apoptosis. *Oncogene*. 1991;6(10):1915-1922.
6. Evan GI, Wyllie AH, Gilbert CS, et al. Induction of apoptosis in fibroblasts by c-myc protein. *Cell*. 1992;69(1):119-128.
7. Murphy DJ, Junttila MR, Pouyet L, et al. Distinct thresholds govern Myc's biological output in vivo. *Cancer Cell*. 2008;14(6):447-457.
8. Vaux DL, Cory S, Adams JM. *Bcl-2* gene promotes haemopoietic cell survival and cooperates with c-*myc* to immortalize pre-B cells. *Nature*. 1988;335(6189):440-442.
9. Strasser A, Harris AW, Bath ML, Cory S. Novel primitive lymphoid tumours induced in transgenic mice by cooperation between *myc* and *bcl-2*. *Nature*. 1990;348(6299):331-333.
10. Amati B, Brooks MW, Levy N, Littlewood TD, Evan GI, Land H. Oncogenic activity of the c-Myc protein requires dimerization with Max. *Cell*. 1993;72(2):233-245.
11. Mao DY, Watson JD, Yan PS, et al. Analysis of Myc bound loci identified by CpG island arrays shows that Max is essential for Myc-dependent repression. *Curr Biol*. 2003;13(10):882-886.
12. Tu WB, Helander S, Pilstål R, et al. Myc and its interactors take shape. *Biochim Biophys Acta*. 2015;1849(5):469-483.
13. Sabò A, Amati B. BRD4 and MYC-clarifying regulatory specificity. *Science*. 2018;360(6390):713-714.
14. Hurlin PJ, Quéva C, Eisenman RN. Mnt, a novel Max-interacting protein is coexpressed with Myc in proliferating cells and mediates repression at Myc binding sites. *Genes Dev*. 1997;11(1):44-58.
15. Meroni G, Reymond A, Alcalay M, et al. Rox, a novel bHLHZip protein expressed in quiescent cells that heterodimerizes with Max, binds a non-canonical E box and acts as a transcriptional repressor. *EMBO J*. 1997;16(10):2892-2906.
16. Walker W, Zhou ZQ, Ota S, Wynshaw-Boris A, Hurlin PJ. Mnt-Max to Myc-Max complex switching regulates cell cycle entry. *J Cell Biol*. 2005;169(3):405-413.
17. Hurlin PJ, Zhou ZQ, Toyo-oka K, et al. Deletion of Mnt leads to disrupted cell cycle control and tumorigenesis. *EMBO J*. 2003;22(18):4584-4596.
18. Nilsson JA, Maclean KH, Keller UB, Pendeville H, Baudino TA, Cleveland JL. Mnt loss triggers Myc transcription targets, proliferation, apoptosis, and transformation. *Mol Cell Biol*. 2004;24(4):1560-1569.
19. Hooker CW, Hurlin PJ. Of Myc and Mnt. *J Cell Sci*. 2006;119(Pt 2):208-216.
20. Toyo-oka K, Bowen TJ, Hirotsune S, et al. Mnt-deficient mammary glands exhibit impaired involution and tumors with characteristics of myc overexpression. *Cancer Res*. 2006;66(11):5565-5573.
21. Dezfouli S, Bakke A, Huang J, Wynshaw-Boris A, Hurlin PJ. Inflammatory disease and lymphomagenesis caused by deletion of the Myc antagonist Mnt in T cells. *Mol Cell Biol*. 2006;26(6):2080-2092.
22. Schaub FX, Dhankani V, Berger AC, et al. Pan-cancer alterations of the MYC oncogene and its proximal network across the Cancer Genome Atlas. *Cell Syst*. 2018;6(3):282-300.
23. Edelmann J, Holzmann K, Miller F, et al. High-resolution genomic profiling of chronic lymphocytic leukemia reveals new recurrent genomic alterations. *Blood*. 2012;120(24):4783-4794.
24. Vermeer MH, van Doorn R, Dijkman R, et al. Novel and highly recurrent chromosomal alterations in Sézary syndrome. *Cancer Res*. 2008;68(8):2689-2698.
25. Link JM, Ota S, Zhou ZQ, Daniel CJ, Sears RC, Hurlin PJ. A critical role for Mnt in Myc-driven T-cell proliferation and oncogenesis. *Proc Natl Acad Sci USA*. 2012;109(48):19685-19690.
26. Campbell KJ, Vandenberg CJ, Anstee NS, Hurlin PJ, Cory S. Mnt modulates Myc-driven lymphomagenesis. *Cell Death Differ*. 2017;24(12):2117-2126.
27. Langdon WY, Harris AW, Cory S, Adams JM. The c-*myc* oncogene perturbs B lymphocyte development in Eμ-*myc* transgenic mice. *Cell*. 1986;47(1):11-18.
28. Harris AW, Pinkert CA, Crawford M, Langdon WY, Brinster RL, Adams JM. The E mu-myc

transgenic mouse. A model for high-incidence spontaneous lymphoma and leukemia of early B cells. *J Exp Med*. 1988;167(2):353-371.

29. Alexander WS, Bernard O, Cory S, Adams JM. Lymphomagenesis in Eμ-myc transgenic mice can involve ras mutations. *Oncogene*. 1989; 4(5):575-581.

30. Eischen CM, Weber JD, Roussel MF, Sherr CJ, Cleveland JL. Disruption of the ARF-Mdm2-p53 tumor suppressor pathway in Myc-induced lymphomagenesis. *Genes Dev*. 1999; 13(20):2658-2669.

31. Egle A, Harris AW, Bouillet P, Cory S. Bim is a suppressor of Myc-induced mouse B cell leukemia. *Proc Natl Acad Sci USA*. 2004; 101(16):6164-6169.

32. O'Connor L, Strasser A, O'Reilly LA, et al. Bim: a novel member of the Bcl-2 family that promotes apoptosis. *EMBO J*. 1998;17(2):384-395.

33. Adams JM, Cory S. The BCL-2 arbiters of apoptosis and their growing role as cancer targets. *Cell Death Differ*. 2018;25(1):27-36.

34. Bouillet P, Cory S, Zhang L-C, Strasser A, Adams JM. Degenerative disorders caused by Bcl-2 deficiency prevented by loss of its BH3-only antagonist Bim. *Dev Cell*. 2001;1(5):645-653.

35. McCormack MP, Forster A, Drynan L, Pannell R, Rabbitts TH. The LMO2 T-cell oncogene is activated via chromosomal translocations or retroviral insertion during gene therapy but has no mandatory role in normal T-cell development. *Mol Cell Biol*. 2003;23(24): 9003-9013.

36. Seibler J, Zevnik B, Küter-Luks B, et al. Rapid generation of inducible mouse mutants. *Nucleic Acids Res*. 2003;31(4):e12.

37. Toyo-oka K, Hirotsune S, Gambello MJ, et al. Loss of the Max-interacting protein Mnt in mice results in decreased viability, defective embryonic growth and craniofacial defects: relevance to Miller-Dieker syndrome. *Hum Mol Genet*. 2004;13(10):1057-1067.

38. Hawkins ED, Duarte D, Akinduro O, et al. T-cell acute leukaemia exhibits dynamic interactions with bone marrow microenvironments. *Nature*. 2016;538(7626):518-522.

39. Duarte D, Hawkins ED, Lo Celso C. The interplay of leukemia cells and the bone marrow microenvironment. *Blood*. 2018;131(14): 1507-1511.

40. Egle A, Harris AW, Bath ML, O'Reilly L, Cory S. VavP-*Bcl2* transgenic mice develop follicular lymphoma preceded by germinal center hyperplasia. *Blood*. 2004;103(6):2276-2283.

41. Herold MJ, Stuchbery R, Mérino D, et al. Impact of conditional deletion of the pro-apoptotic BCL-2 family member BIM in mice. *Cell Death Dis*. 2014;5(10):e1446.

42. Wolyniec K, Shortt J, de Stanchina E, et al. E6AP ubiquitin ligase regulates PML-induced senescence in Myc-driven lymphomagenesis. *Blood*. 2012;120(4):822-832.

43. Duarte D, Hawkins ED, Akinduro O, et al. Inhibition of endosteal vascular niche remodeling rescues hematopoietic stem cell loss in AML. *Cell Stem Cell*. 2018;22(1):64-77.

44. Clark MR, Mandal M, Ochiai K, Singh H. Orchestrating B cell lymphopoiesis through interplay of IL-7 receptor and pre-B cell receptor signalling. *Nat Rev Immunol*. 2014;14(2):69-80.

45. Bouillet P, Metcalf D, Huang DCS, et al. Proapoptotic Bcl-2 relative Bim required for certain apoptotic responses, leukocyte homeostasis, and to preclude autoimmunity. *Science*. 1999;286(5445):1735-1738.

46. Oliver PM, Wang M, Zhu Y, White J, Kappler J, Marrack P. Loss of Bim allows precursor B cell survival but not precursor B cell differentiation in the absence of interleukin 7. *J Exp Med*. 2004;200(9):1179-1187.

47. Huntington ND, Labi V, Cumano A, et al. Loss of the pro-apoptotic BH3-only Bcl-2 family member Bim sustains B lymphopoiesis in the absence of IL-7. *Int Immunol*. 2009;21(6): 715-725.

48. Vassilev LT, Vu BT, Graves B, et al. In vivo activation of the p53 pathway by small-molecule antagonists of MDM2. *Science*. 2004;303(5659):844-848.

49. Heinzel S, Binh Giang T, Kan A, et al. A Myc-dependent division timer complements a cell-death timer to regulate T cell and B cell responses. *Nat Immunol*. 2017;18(1):96-103.

50. Huang CY, Bredemeyer AL, Walker LM, Bassing CH, Sleckman BP. Dynamic regulation of c-Myc proto-oncogene expression during lymphocyte development revealed by a GFP-c-Myc knock-in mouse. *Eur J Immunol*. 2008;38(2):342-349.

51. Rolink AG, Winkler T, Melchers F, Andersson J. Precursor B cell receptor-dependent B cell proliferation and differentiation does not require the bone marrow or fetal liver environment. *J Exp Med*. 2000;191(1):23-32.

52. Grabow S, Delbridge AR, Aubrey BJ, Vandenberg CJ, Strasser A. Loss of a single Mcl-1 allele inhibits MYC-driven lymphomagenesis by sensitizing pro-B cells to apoptosis. *Cell Reports*. 2016;14(10):2337-2347.

53. Kelly GL, Grabow S, Glaser SP, et al. Targeting of MCL-1 kills MYC-driven mouse and human lymphomas even when they bear mutations in p53. *Genes Dev*. 2014;28(1):58-70.

54. Barrans S, Crouch S, Smith A, et al. Rearrangement of MYC is associated with poor prognosis in patients with diffuse large B-cell lymphoma treated in the era of rituximab. *J Clin Oncol*. 2010;28(20):3360-3365.

55. Felsher DW, Bishop JM. Reversible tumorigenesis by MYC in hematopoietic lineages. *Mol Cell*. 1999;4(2):199-207.

56. Meyer N, Penn LZ. Reflecting on 25 years with MYC. *Nat Rev Cancer*. 2008;8(12):976-990.

57. Soucek L, Whitfield JR, Sodir NM, et al. Inhibition of Myc family proteins eradicates KRas-driven lung cancer in mice. *Genes Dev*. 2013;27(5):504-513.

58. Dang CV, Reddy EP, Shokat KM, Soucek L. Drugging the "undruggable" cancer targets. *Nat Rev Cancer*. 2017;17(8):502-508.

59. Chen H, Liu H, Qing G. Targeting oncogenic Myc as a strategy for cancer treatment. *Signal Transduct Target Ther*. 2018;3(1):5.

60. Shortt J, Ott CJ, Johnstone RW, Bradner JE. A chemical probe toolbox for dissecting the cancer epigenome [published correction appears in *Nat Rev Cancer*. 2017;17(4):268]. *Nat Rev Cancer*. 2017;17(3):160-183.

61. Nabet B, Roberts JM, Buckley DL, et al. The dTAG system for immediate and target-specific protein degradation. *Nat Chem Biol*. 2018;14(5):431-441.